



Contents lists available at ScienceDirect

Advanced Powder Technology

journal homepage: www.elsevier.com/locate/apt

Original Research Paper

SiO₂/TiO₂ double-shell hollow particles: Fabrication and UV–Vis spectrum characterization

Wanghui Chen, Chika Takai, Hadi Razavi Khosroshahi, Masayoshi Fuji*, Takashi Shirai

Advanced Ceramics Research Center, Nagoya Institute of Technology, Honmachi 3-101-1, Tajimi, Gifu 507-0033, Japan

ARTICLE INFO

Article history:

Received 16 September 2015

Received in revised form 19 October 2015

Accepted 28 October 2015

Available online xxxx

Keywords:

TiO₂

Hollow particles

Double-shell

SiO₂

UV-vis

Effective-mass model

ABSTRACT

Well-defined SiO₂/TiO₂ double-shell hollow particles (STDSPs) were successfully fabricated by a sol–gel method with avoiding the particle aggregations and the generation of freestanding TiO₂ particles. Comparing with the conventional solid TiO₂ particles, STDSPs showed a novel hollow structure, a much smaller TiO₂ grain size (9 nm), and a larger specific surface area (113 m²/g). In the UV–vis spectrum characterizations, STDSPs showed significant light harvesting capability in both UV- and visible-light range. STDSPs also showed stronger per-weight UV absorbance capability than solid TiO₂ particles and commercial TiO₂ photocatalyst P25, which could be attributed to their novel hollow structure—and thus the absence of light-inaccessible TiO₂ particles. Moreover, we analyzed the narrowed band-gap of STDSPs by the Brus' effective-mass model (EMM).

© 2015 The Society of Powder Technology Japan. Published by Elsevier B.V. and The Society of Powder Technology Japan. All rights reserved.

1. Introduction

Since 1972, when the activity of TiO₂ toward the electrochemical photolysis of water splitting was firstly found by Fujishima and Honda [1], the photoelectrochemical property of TiO₂ has been deeply studied. As a semiconductor, when a photon with energy equal to or greater than the band-gap of TiO₂ was absorbed by TiO₂, an electron in the valence band would conduct an interband transition to the conduction band, and a positive charged hole would accordingly generate in its valence band [2,3]. The formation of photogenerated charge carriers (electrons and holes) derives to the photocatalytic properties of TiO₂. That is, the photogenerated electrons and holes diffuse to the surface of TiO₂ and react with the adsorbed molecular (H₂O, O₂, etc.) to generate some high activity species (hydroxyl radicals, superoxide radical anions, etc.), and then initiate the organic degradation reaction [4–6] or water splitting reaction [7,8].

The photocatalytic property of TiO₂ is influenced by many factors, such as the crystalline structures [9,10], particle size [11], doping elements [12,13], and surface area [14]. Especially, because of their size quantization effect and their large specific surface area, TiO₂ nanoparticles owned their advantages and competitiveness during photocatalytic applications with respect to the bulk TiO₂ [15]. Nevertheless, it was reported that this advantages of

TiO₂ nanoparticles would be weakened by the particle agglomeration. Lin et al. [16] measured the particle size distribution of TiO₂ nanoparticles in aqueous solution which was pre-treated by ultrasound and compared that with their primary particle size which determined by XRD measurements. The results indicated that the agglomeration did take place readily even in a short time. Even worse, the smaller the primary particles were, the faster they aggregated. Obviously, in the practical applications of TiO₂ nanoparticles, a considerable number of TiO₂ primary particles existing inside the secondary particles would be light-inaccessible. Recently, it was found the hollow structure would likely to supply an effective solution for the technique bottleneck in the applications of TiO₂ nanoparticles. It has been reported that the hollow structure could not only supply a high specific surface but also enabled multiple diffractions and reflections of incident light [17]. Therefore, TiO₂ hollow particles could supply much larger area for light adsorption than that of normal solid TiO₂ particles and minimize the proportion of light-inaccessible TiO₂ particles. Kondo et al. [18] found that the catalytic activity of TiO₂ hollow spheres toward gaseous isopropyl alcohol decomposition under UV irradiation was 1.8 times higher than that of the conventional commercial P25 TiO₂ and the dye-sensitized solar cell (DSC) using an electrode of the TiO₂ hollow spheres represented a 2.5 times higher per-weight efficiency toward that of the conventional DSCs of TiO₂. However, such works were rarely reported and even less work referred to the UV–vis spectrum studies of TiO₂ hollow structure, the band gap information as well.

* Corresponding author. Tel.: +81 572 24 8110; fax: +81 572 24 8109.

E-mail address: fuji@nitech.ac.jp (M. Fuji).

In this work, we designed a new TiO₂-based hollow particles–SiO₂/TiO₂ double-shell hollow particles (STDSPs), and focused on their UV–vis spectrum characterizations. The motivation to combine both SiO₂ and TiO₂ in the shells of hollow particles was for sustaining the integration of the shells, since the TiO₂ shells normally showed low mechanical strength. In fact, an additional merit would also be brought by the composition of SiO₂ shell, as suppressing the growth of TiO₂ nanoparticles in size. It is worth noting that the particle aggregation and the generation of free-standing TiO₂ particles were well suppressed by optimizing the experimental parameters in the fabrication process of the STDSPs. In the UV–vis spectrum characterization, we focused on confirming the “light harvesting capability” brought by the hollow structure and comparing the UV-light absorption capability of STDSPs, as well as the band-gap, with that of home-made solid TiO₂ particles (s-TiO₂) and commercial Degussa P25.

2. Experiments

2.1. Materials

CaCO₃ templates were from Yabashi Industries Co., Japan. Tetraethyl orthosilicate (TEOS, 95.0%), Ethanol (99.5%), Ammonia solution (28.0 and 25.0%), Titanium (IV) Tetrabutoxide (TBOT, 95.0%), Acetonitrile (99.5%), and hydrochloric acid (HCl, 35 wt.%) were from Wako Pure Chemical Industries, Ltd. Japan. All the chemicals were used as received and without further purification. DI water was produced by RFD250NB distilled water system (Toyo Roshi Kaisha, Ltd. Japan). P25 TiO₂ powder was provided from Degussa Co., Germany.

2.2. Fabrication of hollow SiO₂ particles (HSPs)

Hollow SiO₂ particles (HSPs) were fabricated by a previously reported modified Stöber method [19]. In a typical process, 10 g CaCO₃ templates were dispersed into a solution containing 300 mL Ethanol, 36 mL water, and 30 mL 25.0 wt% ammonia solution. After 10 min ultrasonic treatment, the uniform CaCO₃ suspension was immediately transferred to a 25 °C thermostatic water bath. Thereafter, 8 mL TEOS was dropped in under vigorous stirring. After 3 h, the reaction was terminated by the addition of excess amount of ethanol. Particles were filtrated and washed with ethanol for several times and then dried under vacuum at 100 °C for overnight. The well dried powder was re-dispersed into 3 M HCl and stirred for 2 h to remove CaCO₃ templates. Finally, the obtained hollow particles were washed with distilled water for several times, and dried under vacuum at 100 °C for overnight.

2.3. Fabrication of STDSPs

STDSPs were synthesized by a sol–gel method using the as-fabricated HSPs as the templates and TBOT as the precursor. Considering the much higher hydrolysis rate of TBOT than that of TEOS, we used acetonitrile to accelerate the mass transfer rate of TBOT and their partial hydrolysates from solvent to the surface of HSPs [20]. During the preparation process, 0.1 g HSPs were dispersed into a solution containing both acetonitrile and ethanol with a volume ratio of 1:3. Then 0.63 mL 28% ammonia solution was added to make the suspension basic. After a 30 min ultrasonic treatment, the uniform suspension was transferred to a 25 °C thermostatic water bath, and then a mixture solution with TBOT, 15 mL Ethanol and 5 mL acetonitrile was dropped in under vigorous stirring. The reaction was allowed to sustain for 3 h. The resultant products were centrifuged under 3000 rpm rotation speed and washed with water and ethanol for 3 times. Thereafter, particles were trans-

ferred into a vacuum oven and dried at 100 °C for 24 h. For comparison, pure TiO₂ solid particles (s-TiO₂) were fabricated by a similar sol–gel method but without the appearance of HSPs. The crystallization (calcination) of TiO₂ was conducted at 600 °C, with the heating rate of 5 °C/min.

2.4. Characterizations

SEM images were taken on JSM-7600F (JEOL Ltd.), and the acceleration voltage was set to 20 kV. XRD patterns were recorded by Ultima IV (Rigaku co.) with Cu K α radiation (40 kV, 40 mA), and the scan step was 0.02°. High resolution transmission electron microscopy (HRTEM) and electron diffraction characterizations were conducted on JEM-2000FX (JEOL Ltd.), and the acceleration voltage was set to 200 kV. The specific surface area of HSPs, STDSPs and s-TiO₂ solid particles was determined by the Brunauer–Emmett–Teller multiplayer nitrogen gas adsorption (BET) method on Belsorp-max-NS (Bel Japan Inc.). X-ray Fluorescence (XRF) analysis was conducted on EDX-7000 (Shimadzu Co. Ltd.). Zetasizer nano-ZS (Malvern Ltd.) was used to conduct the DLS measurements.

The UV–vis diffuse reflectance spectra was recorded by UV-3150 (Shimadzu Co. Ltd.). All the samples were weighed exactly for 0.5 g and then finely spread on the surface of pressed BaSO₄ (Wako Co., Ltd.) powder. During the measurements, the scanning wavelength range was between 300 and 800 nm, slit width was (20) nm, and the scanning speed was set as medium. The respective band gap of each sample could be calculated according to the formula (Eq. (1)) [21]

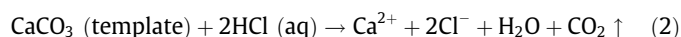
$$(h\nu F(R_{\infty}))^{1/2} = A(h\nu - E_g) \quad (1)$$

where h , ν , A and $F(R_{\infty})$ are Planck's constant, wavelength, proportional constant and Kubelka–Munk function, respectively [16]. In order to simplify the calculation, $(h\nu F(R_{\infty}))^{1/2}$ was plotted against the $h\nu$. A line was drawn tangent to the point of inflection on the $(h\nu - (h\nu F(R_{\infty}))^2)$ curve, and the $h\nu$ value at the point of intersection of the tangent line and the horizontal axis is the band gap E_g value.

3. Results and discussion

3.1. Fabrication of SiO₂/TiO₂ double-shell hollow particles (STDSPs)

Fig. 1a depicts a typical fabrication process of STDSPs, which generally includes two steps. In Step 1st, SiO₂ layers were constructed on the surfaces of CaCO₃ templates by a modified Stöber method [19]—making the hydrolysis and condensation over TEOS conduct under the catalyzing of NH₃. The CaCO₃ templates used in this work were approximate to ellipsoid and with the diameter of 600–700 nm, as seen in Fig. 1b. After the formation of CaCO₃@SiO₂ core–shell particles, the HSPs were further obtained by HCl etching. In this course, HCl penetrated through SiO₂ shells and subsequently etched CaCO₃ templates by conducting the following reaction,



Obviously, void spaces would gradually formed inside CaCO₃@SiO₂ core–shell particles with the on-going penetration and etching process of HCl. To minimize the damage brought by HCl and CO₂ gas penetration to SiO₂ shells, HCl solution with a low concentration (3 M) were used in this work. The SEM observation (Fig. 1c) indicates particles treated by HCl solution for 2 h well maintained the shape and size of CaCO₃ templates, while no fragments and broken particles generated. Furthermore, the high-magnification

Download English Version:

<https://daneshyari.com/en/article/10260337>

Download Persian Version:

<https://daneshyari.com/article/10260337>

[Daneshyari.com](https://daneshyari.com)